Ce:YIG/SOI optical isolator realized by BCB bonding

S.Ghosh[1*], S. Keyvaninia[1], W. Van Roy[2], T. Mizumoto [3], G. Roelkens[1], R. Baets[1]
1. Photonics research group, INTEC department, Ghent University-IMEC, St-Pietersnieuwstraat 41, 9000 Ghent, Belgium.
2. IMEC, Kapeldreef 75, B-3001, Leuven , Belgium
3. Department of Electr. & Electron. Engineering, Tokyo Institute. of Technology, Tokyo, Japan
* email: samir.ghosh@intec.ugent.be

Abstract— **In this paper we demonstrate an optical isolator on a Silicon-on-Insulator waveguide platform realized by the adhesive bonding of Ce:YIG on top of a Mach-Zehnder interferometer. An optical isolation of 25dB is experimentally obtained.**

I. INTRODUCTION

Semiconductor lasers used in optical communication systems are very sensitive to back reflections. In order to achieve stable laser operation an optical isolator typically is required. Given the fast advances in the field of heterogeneous III-V/silicon laser structures, an optical isolator integrated on a silicon waveguide platform is of paramount importance for future high performance silicon photonic integrated circuits. Optical isolation can be achieved by integrating non-reciprocal materials on the silicon waveguide circuits. Ferrimagnetic materials, such as Yttrium Iron Garnet (YIG) or Ce substituted YIG, can be used for this purpose, in combination with an applied external magnetic field. In order to integrate these materials on top of a silicon waveguide circuit, two approaches can be followed. Either the nonreciprocal material is deposited on the SOI wafer using a sputter process [1] or epitaxially grown layers (on a SGGG substrate) are bonded on a silicon waveguide circuit [2]. While the deposition approach is a wafer-scale process, the deposited films suffer from reduced Faraday rotation and large scattering loss. Therefore, in this work we adopt a die-to-wafer bonding technique based on adhesive wafer bonding to integrate Ce:YIG on top of a silicon waveguide circuit. While this was already demonstrated using direct bonding [2], in this work we focus on the use of an adhesive bonding technique. This approach relaxes the surface quality requirements needed to achieve a good bond. This opens a path to integrating the nonreciprocal material after the heterogeneous laser integration process, which will compromise the silicon waveguide circuit surface quality.

II. DESIGN

Commercial fiber-pigtailed bulk isolators use the longitudinal Faraday effect in a polarization rotating ferrimagnetic material such as Yttrium Iron Garnet (YIG), using two polarizers with polarization axes offset by 45° around the garnet, in which the light propagates along the direction of the applied magnetic field. Such an approach is difficult to implement in a high-index contrast photonic integrated circuit, since the waveguide birefringence needs to be brought to zero to obtain substantial optical isolation. Given the fact that the form-birefringence is so strongly dependent on the exact device geometry, this is very difficult to achieve and control. The device presented in this work is based on the non-reciprocal phase shift (NRPS) that TM polarized light experiences when travelling through a garnet containing waveguide structure, when a transverse external magnetic field is applied. This is known as the Voigt effect [3]. This nonreciprocal phase shift can be transformed into a nonreciprocal power transmission by implementing the non-reciprocal phase shifter in a Mach-Zehnder interferometer. The schematic of the realized structure is shown in figure 1.

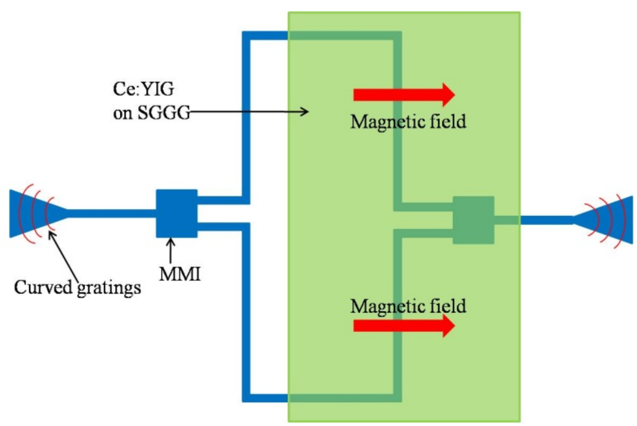

Figure 1 . Schematic layout of the Ce:YIG/SOI optical isolator

Curved diffraction gratings [4] are used to excite the fundamental TM guided mode in a 900nm wide and 220nm high silicon waveguide. The Mach-Zehnder interferometer consists of two 3dB splitter/combiners which are connected through two single mode optical waveguides. The nonreciprocal material overlaps with part of the interferometer, in such a way that the device operates in a push-pull mode, when using a simple NS magnet to apply the transverse magnetic field. In push-pull operation the nonreciprocal phase shift will be opposite in the upper and lower branch of the garnet covered MZI part. The device cross-section in the garnet-covered part of the interferometer is shown in figure 2, also showing the H_y field distribution of the fundamental TM mode at 1.5µm. In order to assess the required length of the nonreciprocal waveguide section, the non-reciprocal phase shift that this mode experiences is calculated as a function of the silicon waveguide thickness and adhesive bonding layer thickness. Since this is a 2D full-vectorial simulation, it gives a good indication of the required length in a 900nm wide waveguide structure. The nonreciprocal phase shift per length unit is obtained by evaluating the integral

$$NRPS = -j\omega\varepsilon_0 \frac{\iint g(x,y) E_x^0\, E_z^0 dxdy}{\iint \left[E_x^0 H_y^0 - E_y^0 H_x^0\right] dxdy}$$

where E_i^0 and H_i^o (i=x,y,z) are the unperturbed field amplitudes of the fundamental TM- mode and *g(x,y)* is the gyrotropy constant which is related to the Faraday rotation coefficient (θ_F) of the nonreciprocal material by

$$g(x, y) = \frac{n\lambda\theta_F}{\pi}$$

where n is the refractive index of the nonreciprocal material and λ is the wavelength of light.

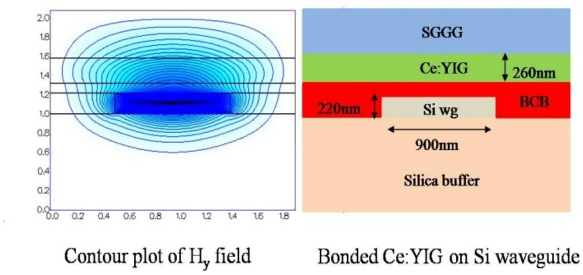

Figure 2 . Waveguide cross-section and mode profile in the garnet-covered section of the isolator

The resulting nonreciprocal phase shift is shown in figure 3, for a 260nm thick Ce:YIG layer (Faraday rotation coefficient: $-4500^0/cm$ at 1.55µm, refractive index: 2.20) on a substituted Gadolinium Gallium Garnet (SGGG) substrate (refractive index:1.94). From this simulation it is clear that compact integrated optical isolators can be realized for sufficiently thin BCB bonding layer thicknesses, since in push-pull operation only a 90° nonreciprocal phase shift per arm of the interferometer is needed. The graph also shows that good control over the BCB bonding layer thickness is required to achieve a reproducible optical isolation.

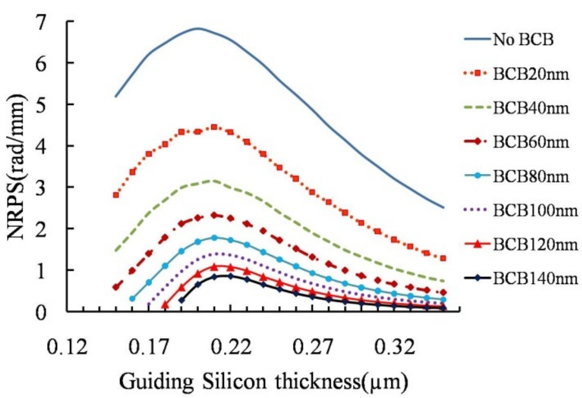

Figure 3. Nonreciprocal phase shift per unit length as a function of BCB bonding layer thickness and silicon waveguide thickness

Since the Mach-Zehnder interferometer is only partially covered with the nonreciprocal material, losses and parasitic reflections can be expected at the interface between the covered and exposed SOI due to the mismatch in the TM-mode field distribution between both regions. These simulated losses and reflections are shown in figure 4, as a function of BCB thickness for a 900nm by 220nm silicon waveguide geometry. It is clear that this loss and associated reflection reduces with increased BCB bonding layer thickness, which leads to a trade-off between device length and insertion loss. Further reduction of the parasitic reflection losses can be achieved by positioning the SGGG die under a small angle to reduce specular reflection into the waveguide.

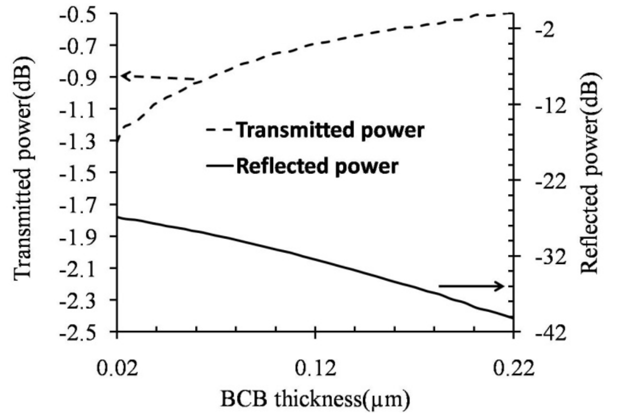

Figure 4. Insertion loss and reflection at the SOI waveguide / Ce:YIG on SOI waveguide interface as a function of BCB bonding layer thickness

In this first demonstration, an asymmetric Mach-Zehnder interferometer with a free spectral range of 7nm was used to ease the observation of the nonreciprocal behavior by measuring the spectral shift in the forward and backward direction. In a real isolator a symmetric Mach-Zehnder interferometer would be used so as to make the operation broadband. The 3dB splitter and combiner were separately designed to account for the presence or absence of the Ce:YIG/SGGG die. The waveguide bend radius used in the design was 60µm, to avoid radiation loss in the Ce:YIG/SGGG.

III. Fabrication

The SOI waveguide circuits were fabricated in a CMOS pilot line using 193nm deep UV lithography. After device fabrication, the SOI dies were cleaned using a standard SC-1 cleaning procedure. Then, AP3000 adhesion promoter is applied. Afterwards, a BCB solution diluted with mesithylene (1:3 v/v) is spin coated at 5000rpm for 50 seconds, after which the SOI die is left on a hot plate at 150°C for 3-4 minutes to evaporate the solvent. The garnet die, grown by sputter epitaxy of Ce:YIG on SGGG is cleaned using acetone and isopropylalcohol. The thickness of the Ce:YIG layer on the SGGG substrate was 260nm. The garnet die is aligned on top of the MZI so that only half of it is covered as depicted in figure 1. Finally, the bonded SOI is cured for about 3 hours using a standard BCB curing recipe. The details about the

BCB bonding technique can be found in [5]. Given the dilution of the BCB and the spin-coating speed, a BCB bonding layer thickness of 100nm can be expected. A photo of the fabricated structure is shown in figure 5. The garnet die size is 2mm by 2mm.

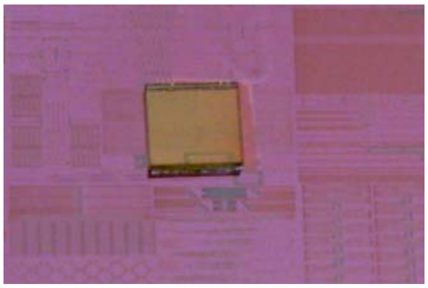

Figure 5 . Photograph of the Ce:YIG die bonded onto an SOI chip

IV. Experimental results

In the experiment, small Neodymium-alloy (NdFeB) permanent magnets are used to create a transverse magnetic field in the Ce:YIG layer. A stack of 3 small magnets is used and is positioned on top of the garnet die. The applied magnetic field is estimated to be sufficient for saturation of the Ce:YIG layer. The transmission characteristic of the Mach-Zehnder interferometer is characterized both in forward and backward direction. Light is injected and extracted using focusing TM grating couplers. The experimentally obtained transmission spectrum of the Mach-Zehnder interferometer is shown in figure 6.

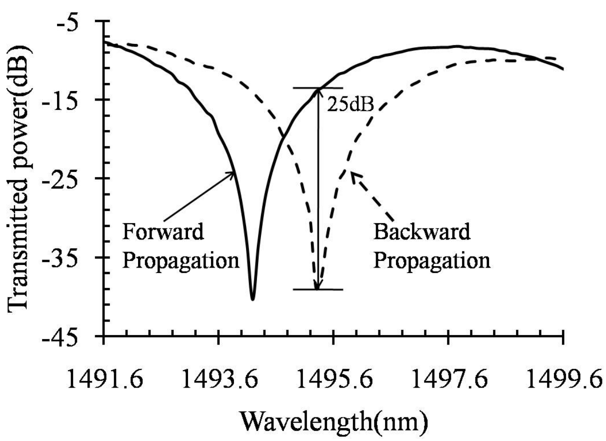

Figure 6. Normalized transmission spectrum of the Mach-Zehnder interferometer

25dB optical isolation is experimentally obtained. A spectral shift of 1.1nm can been observed, which corresponds to a total non-reciprocal phase shift of 28 degrees in the current design. Mapping this experimentally obtained value on the simulation results, indeed a bonding layer thickness of about 100nm is retrieved. The insertion loss at the interface between Ce:YIG covered SOI and plain SOI was experimentally assessed by comparing the transmission on a straight SOI waveguide with that of an SOI waveguide covered with a 2mm YIG die. An excess loss of 4dB was obtained, resulting in 2dB excess loss per interface, provided that the propagation loss in the Ce:YIG/SOI waveguide structure is comparable to that of the plain SOI waveguide. This discrepancy with the simulated loss of 0.8dB indicates either that the interface between the SOI waveguide and the garnet-covered part is not smooth (the garnet dies are diced for bonding) or that the waveguide propagation loss are substantially increased in the garnet covered region. This could be attributed to a horizontal slot waveguide effect, given the Si/BCB/Ce:YIG stack. This enhances the electrical field in the BCB bonding layer, which makes the waveguide geometry more prone to scattering losses.

V. Conclusion

In this paper we present the experimental realization of an optical isolator on a silicon waveguide platform implemented using BCB adhesive bonding. While the device performance can still be improved, this result is promising since it directly opens the path to the dense co-integration of a heterogeneously integrated laser diode and an integrated optical isolator.

References

[1] S. Sung, et.al. , “Integrating Yttrium iron garnet onto nongarnet substrates with faster deposition rates and high reliability”, *Appl.Phys.Lett.*, 87,121111(2005)
[2] Y. Shoji, et.al. , “Magneto-optical isolator with silicon waveguides fabricated by direct bonding”, *Appl.Phys.Lett.*,92, 071117(2008)
[3] R Carey and B W J Thomas, “The theory of the Voigt effect in ferromagnetic materials”, *J. Phys. D: Appl. Phys.*, Vol. 7, 2362-2368, 1974
[4] D. Vermeulen, et.al. , “Efficient Tapering to the Fundamental Quasi-TM mode in Asymmetrical Waveguides”, ECIO, United Kingdom, p. paper WeP16
[5] G. Roelkens, et al., III-V/Si photonics by die-to-wafer bonding, Materials Today, Volume 10,Issues 7-8, p.36-43, 2007.

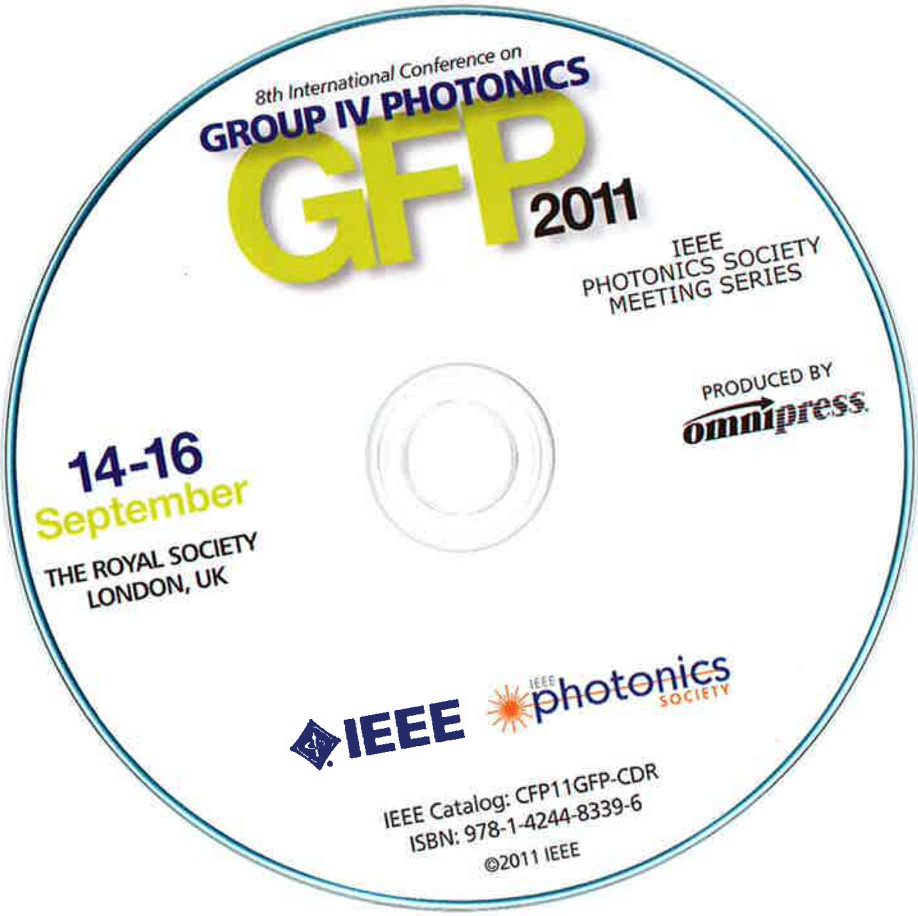
8th International Conference on
GROUP IV PHOTONICS
GFP 2011
IEEE
PHOTONICS SOCIETY
MEETING SERIES
PRODUCED BY
omnipress
14-16
September
THE ROYAL SOCIETY
LONDON, UK
IEEE
IEEE photonics SOCIETY
IEEE Catalog: CFP11GFP-CDR
ISBN: 978-1-4244-8339-6
©2011 IEEE